

Chiral unitary meson–baryon dynamics in the presence of resonances: Elastic pion–nucleon scattering

Ulf-G. Meißner^{#1} and J. A. Oller^{#2}

*Forschungszentrum Jülich, Institut für Kernphysik (Theorie)
D-52425 Jülich, Germany*

Abstract

We develop a novel approach to chiral meson–baryon dynamics incorporating unitarity constraints and explicit resonance fields. It is based on the most general structure of any pion–nucleon partial wave amplitude neglecting the unphysical cuts as derived from the N/D method. This amplitude is then matched to the one–loop heavy baryon chiral perturbation theory result at third order and to tree level exchanges of baryon– and meson states in the s , t and u channels. This generates the left–hand cuts. The unitarization procedure does not involve form factors or regulator functions. The resonance parameters are determined from fits to the S– and P–wave pion–nucleon partial wave amplitudes for energies up to 1.3 GeV. In particular, the $\Delta(1232)$ is accurately reproduced whereas scalar and vector meson couplings are less precisely pinned down. We also obtain a satisfactory description of the πN threshold parameters. Further extensions of this method to coupled channels and the three–flavor case are briefly discussed.

Keywords: Chiral symmetry, unitarity, pion–nucleon scattering, resonances

^{#1}email: Ulf-G.Meissner@fz-juelich.de

^{#2}email: j.a.oller@fz-juelich.de

1 Introduction

There are many reasons why it is interesting to study pion-nucleon scattering. First, in the threshold region, chiral perturbation theory is applicable and thus the chiral structure of QCD can be investigated, see e.g. [1] (and references therein). This very precise method is, however, only applicable in the threshold and in the unphysical region since there the pion momenta are small. At higher energies, additional physics due to the appearance of resonances and coupled channel effects sets in. In fact, the dispersive analysis of pion-nucleon scattering data has been and still is the best method to analyze the properties of the baryon resonances [2] (as long as they couple strongly to the πN system). Many models and approaches of different types have been developed to deal with these phenomena, we just mention the meson-exchange [3] and the extended tree level [4] models. While all these models in general give a good description of the phase shifts (and inelasticities), they are not including the pion loops resulting from the chiral structure of QCD in a systematic fashion (the often employed unitarization schemes or resummation techniques include some classes of these diagrams, but not all). Furthermore, in these references most of the tree level diagrams involving the exchange of meson resonances do not have the momentum dependence required by chiral symmetry. Consequently, it would be interesting to devise a scheme that at low energies exactly reproduces the chiral perturbation theory amplitudes (to a given order in the chiral expansion) but also allows one to work in the resonance region, including also resonance exchange at tree level in conformity with the non-linearly realized chiral symmetry. Such an approach will be developed here. It is similar to the one set up in ref.[5] for meson-meson scattering and will be explained in more detail below. Before doing that, it is worth to stress that this method can easily be extended to the coupled channel case and also to the three-flavor sector, in particular also for the description of kaon-nucleon scattering. While there have been already some successful studies of chiral SU(3) dynamics with coupled channels for this and related processes [6, 7], no attempt has been made so far to match the πN subprocesses to the accurate chiral perturbation theory predictions. Thus, the model presented here can be considered as a first building block for setting up a relativistic coupled channel scheme which fulfills these requirements.

It is known that dispersion theory can be used to match on chiral perturbation theory and thus allows one to extend the range of energies one can consider. Of course, any unitarization scheme is at variance with the power counting underlying an effective field theory like e.g. CHPT. It is, however, not known how to extend such a concept to include resonances (with the exception of the $\Delta(1232)$ isobar, see ref.[8]). On the other hand, unitarization methods allow one to exactly fulfill unitarity (which is only respected perturbatively in CHPT) and can generate S-matrix poles corresponding to resonances. We attempt to combine these concepts in a way that makes best use of these various features. For that, employing the well-known N/D method [9], we derive the most general structure for any πN partial wave amplitude when the unphysical cuts are neglected. Then, similarly as in ref. [10], the unphysical cuts will be treated as a perturbation in a loop expansion with the HBCHPT power counting. Hence, our starting point of no unphysical cuts at all is the zeroth order approach in this scheme from which the first order approach, the one necessary to match with $\mathcal{O}(p^3)$ HBCHPT, is developed. Note that tree level diagrams involving local operators and particle exchanges in all the channels are also included since they do not involve loops. This should be a good starting point for the channels which are dominated by unitarity and the presence of s -, u - or t -channel resonances, like e.g. the P_{33} partial wave which is largely given by the $\Delta(1232)$. The argument is further strengthened by the observation made in ref.[11], namely that the dimension two low-energy constants of the chiral effective πN Lagrangian are saturated by s -, u - and t -channel resonance contributions, most notably

the Δ and the $\rho(770)$. In addition, for the scalar–isoscalar channel one can deduce a certain contribution from a meson with these quantum numbers. In ref.[11], this meson was taken to be a light σ , but in fact only the ratio of the scalar meson–nucleon coupling constant to the scalar meson mass plays a role. We will come back to this point in much more detail below. In addition, we will also include the Roper $N^*(1440)$ resonances which plays a minor but non–negligible role in the energy range we will consider (since we do not calculate inelasticities, we stay below center–of–mass energies of about 1.3 GeV). Note that preferably we should match to a relativistic πN chiral perturbation theory amplitude because in that way one can avoid the difficulties with the HBCHPT approach as detailed in ref.[12]. Such an amplitude, based on a proper power counting, is not yet available but under construction, see ref.[12]. It remains to be seen whether the matching to such an amplitude will lead to better results than the ones presented here.

Our manuscript is organized as follows. In section 2, we collect the formalism necessary to describe elastic pion–nucleon scattering. Section 3 we construct the basic tree level diagrams supplemented by the $\mathcal{O}(p^3)$ HBCHPT loops. In section 4 the unitarization method is discussed and in sections 5 the results are presented. The most relevant conclusions of the work are summarized in section 6.

2 Prelude: Kinematics

In this section, we collect the necessary formalism concerning elastic pion–nucleon scattering. This serves to set our notation and to keep the manuscript self–contained. In the following, we consider the πN scattering amplitude. In the center–of–mass frame (c.m.), the amplitude for the process $\pi(q_1) + N(q_2) \rightarrow \pi(q_2) + N(p_2)$ can be written as (suppressing isospin indices)

$$T(W, t) = \left(\frac{E + m}{2m} \right) \left[g(W, t) + i\vec{\sigma} \cdot (\vec{q}_2 \times \vec{q}_1) h(W, t) \right], \quad (2.1)$$

where \vec{q}_1 and \vec{q}_2 are the three-momenta of the incoming and the outgoing pion, respectively, $W \equiv \sqrt{s}$ is the total c.m. energy, m is the nucleon mass and $t = (q_1 - q_2)^2$ is the invariant momentum transfer squared. Furthermore, $g(W, t)$ refers to the non-spin-flip amplitude and $h(W, t)$ to the spin-flip one. For a given total isospin (I) of the πN system, the partial wave amplitudes $T_{l\pm}^I$, where l refers to the orbital angular momentum and the subscript \pm to the total angular momentum ($J = l \pm 1$), are given in terms of the functions $g(W, t)$ and $h(W, t)$ via

$$T_{l\pm}^I(W) = \frac{E + m}{2} \int_{-1}^1 dz \left[g P_l(z) + |\vec{q}|^2 h (P_{l\pm 1}(z) - z P_l(z)) \right], \quad (2.2)$$

where $z = \cos \theta$, with θ the c.m. angle between the incoming and the outgoing pion, $|\vec{q}|$ is the modulus of the c.m. three-momentum of any of the pions, and $E = \sqrt{m^2 + \vec{q}^2}$ is the c.m. nucleon energy. Note that s , t and u are the Mandelstam variables subject to the constraint $s + t + u = 2m^2 + 2M^2$, with M the pion mass.

As a consequence of unitarity, any partial wave amplitude can also be written in terms of a corresponding phase shift $\delta_{l\pm}^I$ as

$$T_{l\pm}^I(W) = \frac{8\pi W}{|\vec{q}|} \exp(i\delta_{l\pm}^I) \sin \delta_{l\pm}^I. \quad (2.3)$$

This implies the unitarity relation

$$\text{Im } T_{l\pm}^I(W) = \frac{|\vec{q}|}{8\pi W} |T_{l\pm}^I(W)|^2, \quad (2.4)$$

which is valid above threshold and before the opening of any inelastic channel.

The amplitudes $g(W, t)$ and $h(W, t)$ are specially suited for a non-relativistic treatment of the πN scattering, as it is carried out e.g. in Heavy Baryon Chiral Perturbation Theory (HBCHPT) (for a review on HBCHPT see [13] and an update is given in [14]).^{#3} However, in a fully relativistic approach of πN scattering, it is more convenient to work with the invariant amplitudes $A(s, t)$ and $B(s, t)$, which are free of kinematical singularities and are more suited for studying the analytical properties of the scattering amplitude [2]. In terms of the invariant functions $A(s, t)$ and $B(s, t)$, the πN scattering amplitudes are written as:

$$T(W, t) = \bar{u}(p_2, \lambda_2) \left[A(s, t) + \frac{1}{2}(q_2 + q_1)^\mu \gamma_\mu B(s, t) \right] u(p_1, \lambda_1) , \quad (2.5)$$

where the λ_i , appearing in the Dirac spinors, denote the helicities of the incoming/outgoing nucleon. One can derive in a straightforward way the relation between the A , B and g , h amplitudes. From the expressions given in ref. [15] one obtains,

$$\begin{aligned} g &= \frac{1}{2(m+E)^2} \{ (4m(E+m) - t) A + [(W+m)(t+4|\vec{q}|^2) + 4mw(E+m)] B \} , \\ h &= \frac{1}{(m+E)^2} \{ (W+m)B - A \} , \end{aligned} \quad (2.6)$$

with w the c.m. pion energy, $w = W - E$. It is evident from the previous equations that, since the amplitudes $A(s, t)$ and $B(s, t)$ are free of kinematical singularities, the same does not hold for the amplitudes $g(W, t)$ and $h(W, t)$ due to the dependence on $W = \sqrt{s}$. Note that the cut singularities induced by this dependence have nothing to do with the exchange of any particle states. This is the reason why they are called kinematical singularities, in contrast to those due to the exchange of physical particles, which are called dynamical singularities. In the invariant amplitudes $A(s, t)$ and $B(s, t)$, only this latter type of singularity appears.

So far, we have ignored the isospin of the pion ($I_\pi = 1$) and the nucleon ($I_N = 1/2$) fields. Consequently, in πN scattering there are two isospin amplitudes, for total isospin $I=3/2$ and $I=1/2$, respectively. These amplitudes can be written in terms of the $\pi^+ p \rightarrow \pi^+ p$ amplitude, T_1 , and of the one for $\pi^- p \rightarrow \pi^- p$, T_2 , as:

$$\begin{aligned} T_{I=3/2}(W, t) &= T_1(W, t) , \\ T_{I=1/2}(W, t) &= \frac{3}{2}T_2(W, t) - \frac{1}{2}T_1(W, t) . \end{aligned} \quad (2.7)$$

If we denote by $A_1(s, t)$ and $B_1(s, t)$ the invariant amplitudes for $T_1(W, t)$ and by $A_2(s, t)$ and $B_2(s, t)$ the corresponding ones for $T_2(s, t)$ then, by crossing, the following relations arise:

$$\begin{aligned} A_2(s, t) &= +A_1(u, t) , \\ B_2(s, t) &= -B_1(u, t); \end{aligned} \quad (2.8)$$

which allow one to consider just the $\pi^+ p \rightarrow \pi^+ p$ reaction in order to determine the $I = 1/2$ and $3/2$ scattering amplitudes. This is similar to the case of elastic pion-kaon scattering, see e.g. ref.[16].

^{#3}We remind the reader on the remarks made in the introduction on the calculation of pion-nucleon scattering in a relativistic formulation of baryon chiral perturbation theory.

3 Tree level amplitudes and chiral loops

In this section we construct the basic amplitudes which we will unitarize in the next section. First, we consider the tree level contributions to T_1 arising from the lowest order meson-baryon Chiral Perturbation Theory (CHPT) Lagrangian, $\mathcal{L}_{\pi N}^{(1)}$. Then, the exchange of the delta isobar $\Delta(1232)$ and of the $N^*(1440)$ and of meson resonances in the t -channel is also taken into account. Note that beyond leading order, the chiral Lagrangian contains local contact terms of second (and higher) order. In our approach, these will be generated by the explicit contribution from the aforementioned resonances. That this is a sensible starting point is based on the observations made in ref.[11], where the dimension two low-energy constants were fixed from data and it was shown that resonance saturation allows to explain these values. Having set up the tree level Lagrangian, we will then consider the $\mathcal{O}(p^3)$ HBCHPT loop contributions [17, 1] to the different isospin amplitudes taking the results directly from ref.[1].

3.1 Pion–nucleon Born terms

In the two-flavor SU(2) case, the one we are interested in here, the lowest order CHPT pion–nucleon Lagrangian takes the form:

$$\mathcal{L}_{\pi N}^{(1)} = \bar{\Psi}(i\gamma_\mu D^\mu - m + \frac{g_A}{2}\gamma^\mu\gamma_5 u_\mu)\Psi \quad (3.1)$$

In this expression one has to take into account that the nucleon mass, m , and the axial-vector coupling g_A are to be taken in the chiral limit ($m_u = m_d = 0, m_s$ fixed). However, in the following we will use the physical values of these quantities since, when including the chiral loops at $\mathcal{O}(p^3)$ [1], they will be renormalized, up to this order, to their physical values. In the following we will take $g_A = 1.26$ and $m = 938.27$ MeV. The choice of the proton mass is justified because we are only considering the scattering of pions off the proton. From this process we derive the two isospin amplitudes πN scattering, as explained above. On the other hand, the proton p and the neutron n fields are collected in the isospinor Ψ

$$\Psi = \begin{pmatrix} p \\ n \end{pmatrix}, \quad (3.2)$$

the covariant derivative D_μ acting on the nucleon field is given by (note that we do not consider external fields and isospin breaking here)

$$\begin{aligned} D_\mu \Psi &= \partial_\mu \Psi + \Gamma_\mu \Psi, \\ \Gamma_\mu &= \frac{1}{2}[u^\dagger, \partial_\mu u]. \end{aligned} \quad (3.3)$$

Here, $u_\mu = i u^\dagger \partial_\mu U u^\dagger$ and $U = u^2 = \exp[i\tau^j \pi^j / F_\pi]$, where τ^j refers to the Pauli matrices (in isospin space). The tree level diagrams from $\mathcal{L}_{\pi N}^{(1)}$ are depicted in fig.1. The corresponding expressions are:

$$\begin{aligned} T_1^a &= \frac{g_A^2}{4F_\pi^2} \left(4m + \mathcal{R} \frac{u + 3m^2}{u - m^2} \right), \\ T_1^b &= -\frac{\mathcal{R}}{4F_\pi^2}, \end{aligned} \quad (3.4)$$

with $F_\pi = 92.4$ MeV the (weak) decay constant of the pion and $R_\mu = (q_1 + q_2)_\mu$. Note that the direct nucleon exchange diagram does not contribute to $\pi^+ p \rightarrow \pi^+ p$.

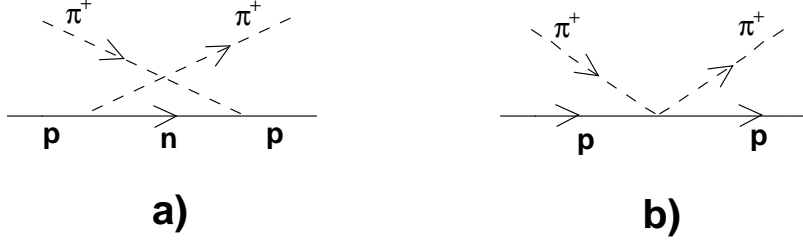


Figure 1: Diagrams from $\mathcal{L}_{\pi N}^{(1)}$: 1.a) Crossed nucleon exchange, 1.b) Seagull.

3.2 Baryon resonances

Next, we consider resonance excitations in the s - (or u -)channel. We treat explicitly the spin-3/2 $\Delta(1232)$ and also the first even-parity excited state of the nucleon, the Roper $N^*(1440)$. Most important for the energy-range we are considering is the $\Delta(1232)$ resonance. It contributes to πN scattering through the $\Delta(1232)$ exchange diagrams, see fig.2. The interactions of the Δ field with pions and nucleons are given by the following effective Lagrangian, which is the leading term of an appropriate chiral invariant interaction [13]

$$\mathcal{L}_{\Delta\pi N} = \frac{g_{\Delta\pi N}}{M} \bar{\Delta}^\nu \vec{T}^\dagger \Theta_{\nu\lambda}(Z) N \partial^\lambda \vec{\pi} + \text{h.c.} , \quad (3.5)$$

where $g_{\Delta\pi N}$ is the $\Delta\pi N$ coupling and $M = 139.57$ is the charged pion mass. This choice is justified since we are considering elastic $\pi^+ p$ scattering. On the other hand, \vec{T} is the $\frac{1}{2} \rightarrow \frac{3}{2}$ isospin transition operator which satisfies

$$\sum_{\lambda_\Delta} T_b \left| \frac{3}{2} \lambda_\Delta \right\rangle \left\langle \frac{3}{2} \lambda_\Delta \right| T_a^\dagger = \delta_{ab} - \frac{1}{3} \tau_b \tau_a . \quad (3.6)$$

Furthermore, the Dirac matrix operator $\Theta_{\mu\nu}(Z)$ is given as

$$\Theta_{\mu\nu}(Z) = g_{\mu\nu} + \left(\frac{1}{2} (1 + 4Z) A + Z \right) \gamma_\mu \gamma_\nu = g_{\mu\nu} - \left(Z + \frac{1}{2} \right) \gamma_\mu \gamma_\nu , \quad (3.7)$$

with the right-hand side valid for $A = -1$. The quantity Z is called an off-shell parameter, which enters the fully relativistic $\Delta\pi N$ vertices. Finally, the spin-3/2 propagator (momentum P , ν to μ) is:

$$-i \frac{\not{P} + m_\Delta}{P^2 - m_\Delta^2} \left(g_{\mu\nu} - \frac{1}{3} \gamma_\mu \gamma_\nu - \frac{2P_\mu P_\nu}{3m_\Delta^2} + \frac{P_\mu \gamma_\nu - P_\nu \gamma_\mu}{3m_\Delta} \right) , \quad (3.8)$$

with m_Δ the mass of the delta resonance, we take $m_\Delta = 1232$ MeV. Note that this mass used in the tree graphs is not necessarily equal to the real part of the S-matrix pole. We will come back to this point later on. For the diagram represented in fig.2a, corresponding to the direct exchange of the Δ , we find

$$\begin{aligned} T_1^{\Delta,a} &= A_1^{\Delta,a} + \frac{1}{2} \not{R} B_1^{\Delta,a} , \\ A_1^{\Delta,a} &= \frac{g_{\Delta\pi N}^2}{6 m_\Delta^2 M^2 (s - m_\Delta^2)} \left\{ m_\Delta^2 m [6 M^2 - 2s - 3t - 4s\kappa^2 + m^2 (2 + 4\kappa^2)] \right. \\ &+ m_\Delta^3 [6 M^2 - 2s - 3t + 4s\kappa - 8s\kappa^2 + 2m^2 (1 - 2\kappa + 4\kappa^2)] \\ &+ 2m_\Delta [-M^4 - M^2 s - 2s^2 \kappa + 4s^2 \kappa^2 + m^2 (M^2 + 2s\kappa - 4s\kappa^2)] \\ &\left. - m [m^4 + M^4 + 2M^2 s + s^2 - 4s^2 \kappa^2 - 2m^2 (M^2 + s - 2s\kappa^2)] \right\} , \end{aligned}$$

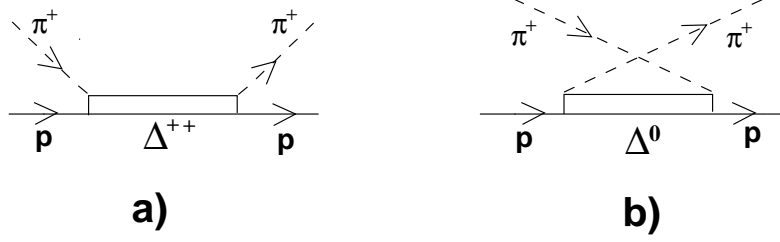


Figure 2: Diagrams with the exchange of the $\Delta(1232)$ resonance.

$$\begin{aligned}
B_1^{\Delta.a} &= \frac{g_{\Delta\pi N}^2}{6 m_{\Delta}^2 M^2 (s - m_{\Delta}^2)} \left\{ -m^4 - (M^2 + s - 2 s \kappa)^2 + 2 m^2 (M^2 + s - 2 s \kappa - 2 s \kappa^2) \right. \\
&+ 4 m_{\Delta}^3 m (1 - 2 \kappa + 4 \kappa^2) + 2 m_{\Delta} m (m^2 - M^2 - s + 4 s \kappa - 8 s \kappa^2) \\
&+ \left. m_{\Delta}^2 [4 M^2 - 3 t - 4 M^2 \kappa - 4 s \kappa + 4 s \kappa^2 + 4 m^2 (1 + \kappa + \kappa^2)] \right\} , \quad (3.9)
\end{aligned}$$

with $\kappa = Z + \frac{1}{2}$. The diagram of fig.2b can we obtained from the former one just by crossing. The result is:

$$\begin{aligned}
A_1^{\Delta.b}(s, t) &= +\frac{1}{3} A_1^{\Delta.a}(u, t) , \\
B_1^{\Delta.b}(s, t) &= -\frac{1}{3} B_1^{\Delta.a}(u, t) . \quad (3.10)
\end{aligned}$$

Let us consider now the exchange of the $N^*(1440)$ Roper resonance, cf. fig.3. Although this resonance is heavier than the $\Delta(1232)$ and not as strongly coupled to the πN system, in ref.[20] it was shown that the Roper octet can have an appreciable interference with the contributions coming from the exchange of scalar resonances. The Lagrangian for the coupling $N^* N \pi$ is [21]

$$\mathcal{L}_{N^* N \pi} = \frac{g_A}{4} \sqrt{R} \bar{\Psi}_{N^*} \gamma_{\mu} \gamma_5 u^{\mu} \Psi_N + \text{h.c.} \quad (3.11)$$

with $\sqrt{R} = 0.53 \pm 0.04$ [21] from the width of the $N^*(1440)$ determined in ref.[22] (note that the often used Breit–Wigner fits to this resonance lead to an appreciably larger width). The resulting amplitude is given by:

$$T_1^{N^*} = \frac{g_A^2 R}{8 F_{\pi}^2 (u - m_R^2)} \left\{ (u - m^2)(m + m_R) + \frac{R}{2} (u + m^2 + 2 m m_R) \right\} \quad (3.12)$$

where $m_R = 1440$ MeV is the mass of the Roper resonance.

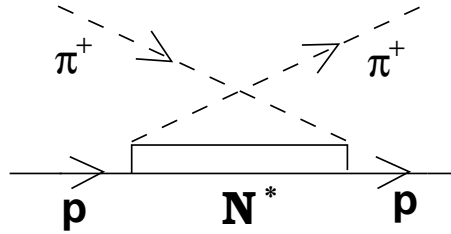


Figure 3: s-channel exchange of the Roper resonance.

3.3 Meson resonances

We now turn to the t -channel exchange of meson resonances. First, we consider the exchange of an isosinglet scalar resonance, cf. fig.4. This state should account for both the contribution of the lightest scalar singlet and octet $I = 0$ states, which in large N_c (where N_c denotes the number of colors) should be degenerate. The SU(2) $S\pi\pi$ interaction can be written as [11]

$$\mathcal{L}_{S\pi\pi} = S [\bar{c}_m \text{Tr}(\chi_+) + \bar{c}_d \text{Tr}(u_\mu u^\mu)] \quad (3.13)$$

with $\chi_+ = \text{diag}(M^2, M^2)$ and the \bar{c}_d, \bar{c}_m are two lowest order coupling constants. In ref.[5], where a simultaneous fit to the all SU(3) related S-wave meson-meson scalar channels was done combining CHPT with the exchanges of resonances in the s -channel via the N/D method, the scalar singlet appears with a mass around 1 GeV and the octet is higher in energy, around 1.35 GeV. In ref. [25] it was shown that the requirement that the tree level $K\pi, K\eta$ and $K\eta'$ scalar form factors vanish at infinity fixes these coupling in terms of the pion decay constant,

$$\bar{c}_d = \bar{c}_m = \frac{F_\pi}{\sqrt{6}}. \quad (3.14)$$

Requiring also the saturation of the $\mathcal{O}(p^4)$ CHPT counterterms for the former couplings, the nonet mass is then fixed to be around 1.2 GeV, which lies in an intermediate value between the singlet and octet mass given in ref.[5]. The well-known $\sigma(550)$ meson, see e.g. refs.[26, 5, 27] should be considered as a reflection of the strong S-wave $\pi\pi$ interactions, loop physics and hence subleading in large N_c counting rules (this has already been stressed a long time ago, see [28]). Other QCD inspired approaches, which also establish that the lightest preexisting scalar meson should be around 1 GeV, are collected in refs.[29, 30]. While the contributions of a preexisting scalar resonance appear at $\mathcal{O}(p^2)$ in the chiral counting, the crossed pions loops, and hence their associated σ pole, begins at $\mathcal{O}(p^3)$. The coupling of the scalar $I = 0$ resonance to the nucleon is calculated easily from the Lagrangian

$$\mathcal{L}_{SNN} = -g_s \bar{\Psi} \Psi . \quad (3.15)$$

From eqs.(3.13),(3.15) we obtain the scalar meson exchange contribution to πN scattering,

$$T_1^S = -2g_S \frac{\bar{c}_m 2M^2 + \bar{c}_d (t - 2M^2)}{F_\pi^2 (t - M_S^2)} \quad (3.16)$$

with M_S the mass of the scalar resonance.

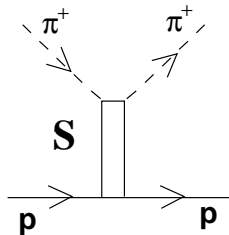


Figure 4: t -channel exchange of an isosinglet resonance, S .

Next, we consider the exchange of the $\rho(770)$ meson in the t -channel, fig.5. Following refs.[18, 19], we consider the tensor representation for the vector fields. In this way, we generate terms in the chiral expansion of the pion-nucleon scattering amplitude that begin at $\mathcal{O}(p^2)$. On the other hand, if we were to use the vector representation, the contributions from the exchange of the ρ would begin to appear only for orders higher than $\mathcal{O}(p^2)$.

Consequently, extra local contact terms would be needed in order to make both representations, vector and tensor, equivalent [23, 19]. The tensor field representation is most useful in constructing chiral invariant building blocks for spin-1 mesons coupled to nucleons, pions and external fields (like e.g. photons). The $\rho\pi^+\pi^-$ vertex can be obtained from the Lagrangian [18]

$$\mathcal{L}_{V\phi\phi} = i\frac{G_V}{\sqrt{2}}\text{Tr}[W_{\mu\nu}u^\mu u^\nu] , \quad (3.17)$$

where $W_{\mu\nu}$ refers to the tensor field representing the octet of the lowest-lying vector resonances,

$$W_{\mu\nu} = \begin{pmatrix} \frac{\rho^0}{\sqrt{2}} + \frac{\omega_8}{\sqrt{6}} & \rho^+ & K^{*+} \\ \rho^- & -\frac{\rho^0}{\sqrt{2}} + \frac{\omega_8}{\sqrt{6}} & K^{*0} \\ K^{*-} & \bar{K}^{*0} & -\frac{2\omega_8}{\sqrt{6}} \end{pmatrix}_{\mu\nu} \quad (3.18)$$

such that

$$\langle 0|W_{\mu\nu}|V, p\rangle = iM_V^{-1}[p_\mu\epsilon_\nu(p) - p_\nu\epsilon_\mu(p)] , \quad (3.19)$$

with $\epsilon_\mu(p)$ the usual polarization vector for the vector state $|V, p\rangle$ with a mass in the chiral limit of $M_V \approx M_\rho = 770$ MeV [18]. The propagator is given by

$$\frac{M_V^{-2}}{M_V^2 - p^2 - i\epsilon} [g_{\mu\rho}g_{\nu\sigma}(M_V^2 - p^2) + g_{\mu\rho}p_\nu p_\sigma - g_{\mu\sigma}p_\nu p_\rho - (\mu \leftrightarrow \nu)] . \quad (3.20)$$

The coupling G_V can be obtained from the decay $\rho \rightarrow 2\pi$ and one obtains $G_V = 69$ MeV. Another possible way of determining G_V is from fitting the charge radius of the pion. That leads to a reduced value of $G_V = 53$ MeV [24]. We will distinguish below between both values when we present our results. One has to take into account that in ref. [18, 19] an SU(3) notation is considered. We will also use this three-flavor notation to work out the ρ -couplings. The only difference for our considerations is that the Pauli matrices, τ^i , are changed to the Gell-Mann matrices λ^i . In this way the SU(3) representation of the Goldstone boson octet reads

$$U = \exp\left(i\frac{\lambda^j\phi^j}{F_\pi}\right) = \begin{pmatrix} \frac{\pi^0}{\sqrt{2}} + \frac{\eta_8}{\sqrt{6}} & \pi^+ & K^+ \\ \pi^- & -\frac{\pi^0}{\sqrt{2}} + \frac{\eta_8}{\sqrt{6}} & K^0 \\ K^- & \bar{K}^0 & -\frac{2\eta_8}{\sqrt{6}} \end{pmatrix} . \quad (3.21)$$

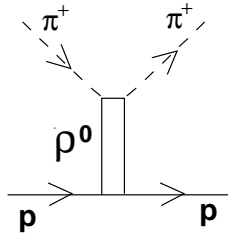


Figure 5: t-channel exchange of the $\rho(770)$ resonance.

On the other hand, the ρNN vertex can be inferred from ref.[19] from the general vector to baryon octet coupling via

$$\begin{aligned} \mathcal{L}_{VNN} &= R_{D/F}\text{Tr}[\bar{B}\sigma^{\mu\nu}(W_{\mu\nu}, B)] + S_{D/F}\text{Tr}[\bar{B}\gamma^\mu(\partial^\nu W_{\mu\nu}, B)] \\ &+ T_{D/F}\text{Tr}[\bar{B}\gamma^\mu(\partial_\lambda W_{\mu\nu}, \partial^\lambda\partial^\nu B)] + U_{D/F}\text{Tr}[\bar{B}\sigma^{\lambda\nu}(W_{\mu\nu}, \partial_\lambda\partial^\mu B)] . \end{aligned} \quad (3.22)$$

Here, the symbol (A, B) denotes either the commutator, $(A, B) = [A, B]$, or the anticommutator, $(A, B) = \{A, B\}$. In the first case, the coupling constant has the subscript F , in the second one the subscript D applies. For instance, the first term in the previous equation thus means

$$R_D Tr[\bar{B}\sigma^{\mu\nu}\{W_{\mu\nu}, B\}] + R_F Tr[\bar{B}\sigma^{\mu\nu}[W_{\mu\nu}, B]] . \quad (3.23)$$

From the Lagrangians given in eqs.(3.17) and (3.22), one obtains for the diagram depicted in fig.5:

$$T_1^\rho = \frac{2G_V\sqrt{2}}{F_\pi^2(M_\rho^2 - t)} \left\{ R_+ \frac{u-s}{2} + \frac{\mathcal{R}}{2} \left[2mR_+ + \frac{t}{2} \left(S_+ - \frac{mU_+}{2} \right) - \frac{t^2 T_+}{8} \right] \right\} , \quad (3.24)$$

with $R_+ = R_D + R_F$ and analogously for S_+ , U_+ and T_+ . All the former unknown parameters, except T_+ , can be recast in terms of more familiar ones, by comparing eq.(3.24) with the result that one would obtain by making use of the standard vector representation for the ρ meson. In this case, instead of the Lagrangian given in eq.(3.22), one has:

$$\mathcal{L}_{\rho NN} = \frac{1}{2} g_{\rho NN} \bar{\Psi} \left[\gamma^\mu \vec{\rho}_\mu \vec{\tau} - \frac{\kappa_\rho}{2m} \sigma^{\mu\nu} \partial_\nu \vec{\rho}_\mu \vec{\tau} \right] \Psi , \quad (3.25)$$

with $g_{\rho NN}$ the vector coupling of the ρ to two nucleons and κ_ρ the ratio between the tensor and the vector couplings. After these preliminaries, the final expression that we obtain for the ρ -exchange contribution is given by:

$$\begin{aligned} T_1^\rho &= \frac{t G_V g_{\rho NN}}{M_\rho F_\pi^2 (t - M_\rho^2)} \left(\frac{1 + \kappa_\rho}{2} \mathcal{R} + \frac{u-s}{4m} \kappa_\rho \right) \\ &- \frac{g_{\rho NN} \kappa_\rho G_V}{F_\pi^2 M_\rho} \left(\frac{\mathcal{R}}{2} + \frac{u-s}{4m} \right) + \frac{t^2 \sqrt{2} G_V}{4 F_\pi^2 (t - M_\rho^2)} T_+ . \end{aligned} \quad (3.26)$$

Note that the coupling $\sim t^2 T_+$ has not been considered before although it is solely based on chiral symmetry. Its relevance for the ρ NN phenomenology will be discussed below.

3.4 Chiral pion loops

As explained in detail in the introduction, we consider here the $\mathcal{O}(p^3)$ one-loop contributions obtained in the framework of heavy baryon chiral perturbation theory. After renormalizing all the bare parameters, these loop contributions are given in ref. [1]. Their contributions to the spin-non-flip and spin-flip amplitudes with given total isospin ($I = 3/2$ or $1/2$), $g_{3/2}$, $g_{1/2}$ and $h_{3/2}$, $h_{1/2}$ are:

$$\begin{aligned} g_{3/2\text{loop}} &= g_{\text{loop}}^+ - g_{\text{loop}}^- \\ g_{1/2\text{loop}} &= g_{\text{loop}}^+ + 2 g_{\text{loop}}^- \end{aligned} \quad (3.27)$$

where we have followed the notation of ref. [1] to denote their calculated loop functions. For the $h_{3/2\text{loop}}$ and $h_{1/2\text{loop}}$ functions analogous relations with the functions h_{loop}^+ , h_{loop}^- as the ones shown in eq.(3.27) hold.

4 Unitarization

As a consequence of eqs.(2.2) and (2.6), any π N partial wave amplitude has besides the dynamical cuts, which are due to the exchange of particle states in the s -, t - or u - channel,

further kinematical singularities arising from the \sqrt{s} -dependence in eq.(2.6). In the following, we will consider a partial wave amplitude as a function of W , instead of s , and hence the kinematical singularities disappear. The dynamical cuts are usually divided into two classes: the physical or unitarity cut and the unphysical cuts. The physical cut is required by unitarity, eq.(2.4), and the unphysical cuts are due to the exchanges of particles in the crossed channels. A more detailed discussion of the ideas underlying this approach are given in ref.[5]. Here, we are concerned with the extension of such a scheme to the pion–nucleon sector.

4.1 The right–hand cut

We consider first the physical or right–hand cut and neglect, for the moment, the unphysical ones. In order to obtain a unitarized πN amplitude, we follow ref.[5], in which meson–meson scattering was considered. In this work, making use of the N/D method [9], the most general structure of a meson–meson partial wave amplitude, when no unphysical cuts are considered, is given. If we denote by $T_l(s)$ a meson–meson partial wave with orbital angular momentum l the central result of ref.[5] takes the form:

$$\begin{aligned} T_l(s) &= \frac{N(s)}{D(s)} \\ N(s) &= 1 \\ D(s) &= \sum_i \frac{R_i}{s - s_i} + a(s_0) - \frac{s - s_0}{\pi} \int_{s_{\text{thr}}}^{\infty} ds' \frac{\rho(s')}{(s' - s)(s' - s_0)}. \end{aligned} \quad (4.1)$$

Here $\rho(s) = |\vec{q}|/(8\pi\sqrt{s})$, see eq. (2.4), s_{thr} is the value of s for the threshold of the reaction, s_0 is the subtraction point, $a(s_0)$ a subtraction constant and each pole of the sum is referred to as a CDD pole after ref.[31], with s_i the pole position and R_i the corresponding residue. Note that a CDD pole is a pole of the $D(s)$ function so that it corresponds to a zero of the partial wave $T_l(s)$.

In order to translate the result of eq.(4.1) to the πN case, we first consider how the right–hand cut, given by the integral in eq.(4.1), looks like in the complex W -plane. Note that because $W = \sqrt{s}$ and since the square root is a double–valued function, we will have two cuts in the W -plane. One of these cuts extends from $W > W_{\text{thr}} = M + m$ to $+\infty$ and the other one from $-\infty$ to $-W_{\text{thr}}$. Therefore, the contour of integration in the complex s -plane used in ref.[5] to obtain eq.(4.1), Fig.6, transforms in the W -plane to the one shown in fig.7. In this last figure, each line is denoted by two numbers i, j : i refers to the corresponding line in Fig.6 and $j = 1$ means first sheet for $W = \sqrt{s}$ ($\text{Im}W > 0$) and $j = 2$ refers to the second one ($\text{Im}W < 0$). Then the dispersion integral in the W -plane for $D(W)$, with a subtraction in W_0 , will be:

$$\begin{aligned} &\frac{W - W_0}{2\pi i} \left\{ \int_{W_{\text{thr}}}^{\infty} dW' \frac{D(W')_{11}}{(W' - W)(W' - W_0)} - \int_{W_{\text{thr}}}^{\infty} dW' \frac{D(W')_{22}}{(W' - W)(W' - W_0)} \right. \\ &+ \left. \int_{W_{\text{thr}}}^{\infty} dW' \frac{D(-W')_{21}}{(W' + W)(W' + W_0)} - \int_{W_{\text{thr}}}^{\infty} dW' \frac{D(-W')_{12}}{(W' + W_0)(W' + W)} \right\} \end{aligned} \quad (4.2)$$

where we have indicated by a subindex ij the line in Fig.7 over which the integral has to be taken. Making use in the former expression of the fact that $T(W) = T^*(W^*)$, where $*$ means complex conjugation, we then have

$$\frac{W - W_0}{\pi} \left\{ \int_{W_{\text{thr}}}^{\infty} dW' \left[\frac{\text{Im}D(W')_{11}}{(W' - W)(W' - W_0)} + \frac{\text{Im}D(-W')_{21}}{(W' + W)(W' + W_0)} \right] \right\} \quad (4.3)$$

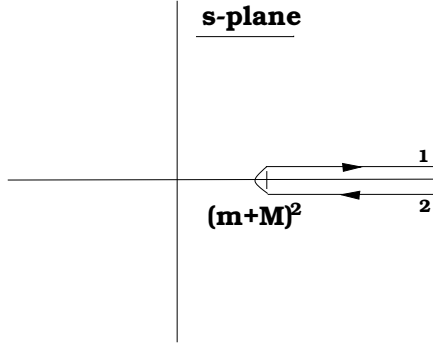


Figure 6: Contour of integration for the Cauchy representation of $D(s)$ eq. (4.1). The enclosing circle extending to infinity is not shown.

Since the line denoted by 21 in Fig.7 corresponds to the line 2 in fig.6, then

$$\text{Im}D(-W')_{21} = -\text{Im}D(W')_{11} = \rho(W') \quad (4.4)$$

and hence we finally have

$$\begin{aligned} & \frac{W - W_0}{\pi} \int_{W_{\text{thr}}}^{\infty} dW' \text{Im}D(W')_{11} \left[\frac{1}{(W' - W)(W' - W_0)} - \frac{1}{(W' + W)(W' + W_0)} \right] \\ = & -\frac{s - s_0}{\pi} \int_{s_{\text{thr}}}^{\infty} ds' \frac{\rho(s')}{(s' - s)(s' - s_0)}, \end{aligned} \quad (4.5)$$

with $s_0 = W_0^2$ and $s' = W'^2$. Thus, we recover the same integral as in eq.(4.1) but this time in the complex W -plane. The remaining terms in eq.(4.1) are not altered: the subtraction constant is, of course, also present in the W -variable case, and the CDD poles will be now in the form $R'_i/(W - W_i)$. Note that, as stated above, these poles represent just zeros of the $T_{l\pm}^I(W)$ partial wave and then have to appear as poles of the $D(W)$ function but now in the W -variable. Note that a complex CDD pole in the s -variable gives rise to four poles in the W -variable. Hence, instead of eq.(4.1) we will have for any πN partial wave $T_{l\pm}^I(W)$:

$$T_{l\pm}^I(W) = \left[\sum_i \frac{R'_i}{W - W_i} + a(s_0) - \frac{s - s_0}{\pi} \int_{s_{\text{thr}}}^{\infty} ds' \frac{\rho(s')}{(s' - s)(s' - s_0)} \right]^{-1} \quad (4.6)$$

It is important to stress that in what follows we will fix the subtraction constant at a point s_0 where it is real. This, however, is done for convenience and need not be done. For $a(s_0)$ to be real, we have $s_0 \leq s_{\text{thr}}$, with s_{thr} the threshold of the reaction under consideration. Note also that eq.(4.6) allows to accommodate the possible pole of $T_{l\pm}^I(W)$ at $W = 0$, due to the kinematical singularities [2], which give rise to a $1/W$ factor in our definition of the partial wave amplitudes.

A connection with the large N_c limit [32] is very enlightening. In this limit of QCD the dominant terms of any meson-baryon amplitude are of order $\mathcal{O}(N_c^0)$ and given by the local terms and pole contributions. These are obtained in eq.(4.6) by the inverse of the CDD poles and the leading piece of the subtraction constant, which are of order $\mathcal{O}(N_c^0)$. Note that the integral in this equation, which contains the unitarity loops in the s -channel, is of order $\mathcal{O}(N_c^{-1})$ and hence is subleading in the large N_c counting, as expected. As a consequence, we split the subtraction constant in two pieces:

$$a(s_0) = a^L + a^{SL}(s_0) \quad (4.7)$$

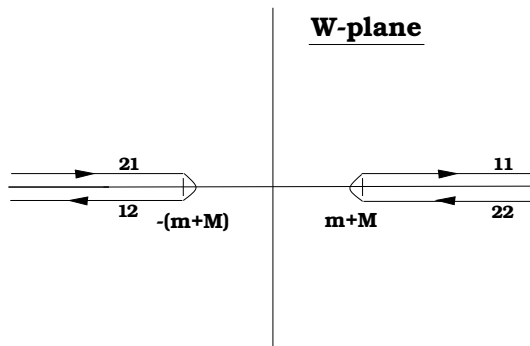


Figure 7: Contour of integration for the Cauchy representation of $D(W)$ eq. (4.6). The enclosing circle extending to infinity is not shown.

where a^L is $\mathcal{O}(N_c^0)$ and independent of the subtraction point s_0 , while $a^{SL}(s_0)$ is $\mathcal{O}(N_c^{-1})$ and is linked to the integral so that their sum is independent of the subtraction point s_0 . Therefore, we introduce the function $g(s)$

$$g(s) = a^{SL}(s_0) - \frac{1}{\pi} \int_{s_{\text{thr}}}^{\infty} ds' \frac{\rho(s')}{(s' - s)(s' - s_0)}. \quad (4.8)$$

On the other hand, we also need the K function

$$K(W) = \left[\sum_i \frac{R'_i}{W - W'_i} + a^L \right]^{-1}. \quad (4.9)$$

Hence, in the absence of unphysical cuts, we can write

$$T_{l\pm}^I = [K(W)^{-1} + g(s)]^{-1} = \frac{K(W)}{1 + K(W)g(s)}, \quad (4.10)$$

in close analogy with a K -matrix formalism. In this derivation we have considered the isospin limit. The extension of this framework to include strong isospin violation is based on a coupled channel formalism as detailed in ref. [5]. Further isospin breaking due to electromagnetic effects is harder to include and will not be considered in what follows.

4.2 The left-hand cut

We have discussed in detail the case of no unphysical cuts since we will take this case as our starting point. The unphysical cuts will be treated in a perturbative way. The perturbation will be done in a chiral loop expansion of the unphysical cuts. In this way, our final calculation will include their contributions up to one loop calculated at $\mathcal{O}(p^3)$ in HBCHPT.^{#4} This way of proceeding has already been used in ref.[10] to study the strong $W_L W_L$ scattering in the strongly interacting Higgs sector and is also being used in ref.[25] to study the $K\pi$, $K\eta'$ S-wave scattering.

Let us now discuss in detail our treatment of the left-hand cuts. Denote by $T_{\text{tree+loop}}^{Il\pm}$ any πN partial wave amplitude resulting from the contributions discussed in sect. 3. If we

^{#4}Strictly speaking the HBCHPT counting is referred to the $g(W, t)$ and $h(W, t)$ functions because the coefficient $(E + m)/2$ in front of eq.(2.2) is not expanded. This is based on the fact that for a proper wavefunction renormalization and matching to the relativistic theory, one should keep this prefactor as it is given here. For a discussion on these issues, see ref.[33].

assume the saturation of the HBCHPT counterterms up to $\mathcal{O}(p^3)$ by resonance exchange and perform a non-relativistic expansion of $T_{\text{tree+loop}}^{Il\pm}$, we would recover the HBCHPT amplitude up to $\mathcal{O}(p^3)$ given in ref.[1]. We now write

$$T_{l\pm}^I(W) = \frac{N(W)}{D(W)} = \frac{N(W)}{1 + N(W)g(s)} \quad (4.11)$$

with $N(W) = K(W)(1 + \delta N(W))$. For the case of not including any unphysical contributions, i.e. $\delta N(W) = 0$, we recover eq.(4.10). We expand this representation of the partial wave amplitudes in order to reproduce the one loop $\mathcal{O}(p^3)$ HBCHPT result $T_{\text{tree+loop}}^{Il\pm}$:

$$T_{\text{tree+loop}}^{Il\pm}(W) = N(W) - N_1(W)^2 g(s) , \quad (4.12)$$

where $N_1(W)$ is the $\mathcal{O}(p)$ contribution of $N(W)$ and is given by the lowest order HBCHPT amplitudes. Consequently

$$N(W) = T_{\text{tree+loop}}^{Il\pm}(W) + N_1(W)^2 g(s) . \quad (4.13)$$

We note that $T_{\text{tree+loop}}^{Il\pm}$ satisfies perturbative unitarity up to $\mathcal{O}(p^3)$ in the HBCHPT chiral counting, which can be traced back to the proper wave function renormalization of the tree graphs. However, to assure exact unitarity also for the loop graphs (which is of higher order in HBCHPT), we have to multiply $g(s)$ in the previous equation by a correction factor, $\varrho = (2W)/(E + m) = 1 + \mathcal{O}(p^2)$. This assures a complete matching of the heavy baryon amplitude to the relativistic one with respect to the constraints from unitarity. Stated differently, if would not multiply the function $g(s)$ by ϱ , then the exact unitarity would be lost. Note that from the last equation and in eq.(4.11), the $N(W)$ and the $D(W)$ functions satisfy the N/D equations up to the same order than our input $T_{\text{tree+loop}}^{Il\pm}(W)$, that is, up to one loop calculated at $\mathcal{O}(p^3)$ in HBCHPT. On the other hand, the D function satisfies them exactly for the right-hand cut. As a result, our final expression for any partial wave, eqs.(4.11) and (4.13), satisfies unitarity to all orders. We note that the low-energy representation could be further improved by matching to the fourth order HBCHPT amplitude, which should be available in the near future.

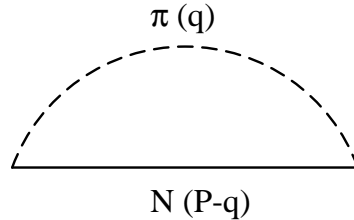


Figure 8: Loop graph corresponding to the function $g(s)$.

Before finishing this section, we give an alternative expression for $g(s)$ more suited than eq.(4.8) for a direct comparison with HBCHPT. This new expression is derived making use of dimensional regularization. Since the function $g(s)$ corresponds, up to a constant, to the loop graph with one pion and one nucleon propagator, see fig.8, we can write:

$$g(s) = \bar{a}^{SL}(\lambda) + \frac{1}{(4\pi)^2} \left\{ -1 - \frac{w}{m} \log \frac{M^2}{\lambda^2} + \log \frac{M^2}{\lambda^2} - \frac{m^2 - M^2 + s}{2s} \log \frac{M^2}{m^2} - \frac{|\vec{q}|}{W} \log \left(\frac{m^2 + M^2 - s + 2W|\vec{q}|}{m^2 + M^2 - s - 2W|\vec{q}|} \right) \right\} . \quad (4.14)$$

In the former expression we have subtracted the piece

$$\frac{w}{(4\pi m)^2} \log \frac{M^2}{\lambda^2} \quad (4.15)$$

since this, together with the singular terms stemming from dimensional regularization:

$$L(\lambda) = \frac{\lambda^{d-4}}{16\pi^2} \left\{ \frac{1}{d-4} - \frac{1}{2} [\ln(4\pi) + \Gamma' + 1] \right\}, \quad (4.16)$$

with d the number of space–time dimensions, is reabsorbed in the $\mathcal{O}(p^3)$ HBCHPT counterterms [1]. On the other hand, the subtraction constant \bar{a}^{SL} is fixed such that for a value of W below threshold and in its neighborhood, $g(s) = 0$. Note again that since we require \bar{a}^{SL} to be real, this matching has to be performed at or below the physical threshold, $s_{\text{thr}} = (m + M)^2$. It is known that the HBCHPT converges best in certain unphysical regions (but not in all), see e.g. ref.[15]. Therefore, in this energy domain we have $T_{l\pm}^I = T_{\text{tree+loop}}^{Il\pm} = T_{\text{HBCHPT}}^{Il\pm} + \mathcal{O}(p^4)$, which should be an accurate estimate of the true value of the partial wave since around threshold HBCHPT to $\mathcal{O}(p^3)$ is convergent. We have fixed the regularization scale at $\lambda = m$. Note that a change in the scale λ is reabsorbed in a change of the constant \bar{a}^{SL} , such that at the end the value of $g(s)$ is unaltered.

5 Results

In this section, we show and discuss the results. First, we explain how we have determined the parameters and which of these are strongly constrained by our fits. Then, we show some representative fits to the low–lying partial waves, exhibiting in particular the dependence on some of the coupling constants and mass parameters.

5.1 Fitting procedure and parameters

First, since we do not consider inelasticities, we restrict the fits to a c.m. energy of $W \leq 1.3$ GeV. We fit the two S– and the four P–waves, these are S_{11}, S_{31} and P_{11}, P_{13}, P_{31} and P_{33} , respectively. The fits are based on the Karlsruhe–Helsinki KA84 [38] and the VPI SM95 [39] phase shift analyses. These PWAs do not give errors. One could assume an overall uncertainty of a few percent, but in that way the smaller partial waves would be too strongly weighted. Also, there should be some overall systematic error. To deal with these two effects and to give proper weight to the large partial waves (in particular the P_{33}), we work with an error function for each partial wave of the form

$$\text{err}(\delta) = \sqrt{e_s^2 + 0.0025 \delta^2}, \quad (5.1)$$

with $e_s = 0$ or $e_s = \sqrt{2}$ and the phase shift δ is given in radians. In this was a systematic error of e_s and a statistical one of a 5% are added in quadrature. As will be shown in more detail below, the choice $e_s = 0$ gives more weight to the threshold region whereas for $e_s = \sqrt{2}$ we obtain a very precise description at higher energies, in particular for the Δ , and an overall better fit for the experimental data up to $W = 1.3$ GeV. Explicit figures for the fits are displayed in the next section. We now enumerate and discuss the parameters, which are essentially coupling constants and masses of the excited baryon and meson resonances. Fitting these parameters can be compared to a study in CHPT, where one fits the pertinent LECs. Clearly, for very low energies, this is analogous to assume resonance saturation of the LECs, which appears to be a sensible approach. However, due to the explicit propagators, a

fitting procedure as performed here, which is also unitary, can be extended to energies where HBCHPT can not work any more. We have performed various types of fits, leaving these parameters completely unlimited or prescribing limits on some of the parameters based on other phenomenological observations. These we will discuss in detail in what follows. Clearly, not limiting certain parameters can lead to rather large (unphysical) values for them. However, what we mostly can determine are products of couplings (with respect to some reference mass) and these normalized products always come out in very limited and sensible ranges. We should also stress that since our approach does not involve form factors, one has to be careful to compare our results to the ones obtained e.g. in meson–exchange models. Having made these general remarks, consider now the various fits.

First, we discuss the generic results for the case $e_s = \sqrt{2}$. For the $\Delta(1232)$, we have the coupling constant and the parameter Z . We find that independently of how we perform the fits, $Z \simeq -0.1$ and $g_{\pi\Delta N} = 2.05$. Note that the values for Z are well within the ranges of previous determinations, cf. refs.[34, 35]. We note that the standard spin–isospin SU(4) using the Goldberger-Treiman relation, $g_{\pi NN} = g_A m / F_\pi$, leads to (we normalize the coupling in terms of the charged pion mass)

$$g_{\pi\Delta N} = \frac{3g_A}{2\sqrt{2}F_\pi} = 2.01/M . \quad (5.2)$$

This means that the Delta parameters are well determined by the fit. We have also determined the complex pole in the energy plane corresponding to the P_{33} resonance and find

$$(m_\Delta, \Gamma_\Delta/2) = (1210, 53) \text{ MeV} , \quad (5.3)$$

in perfect agreement with dispersive analyses of pion–nucleon scattering [2] or pion photoproduction [40]. For the energy range we consider, the Roper only plays a role in the P_{11} partial wave. We have performed fits with and without Roper. Including the Roper, we find that for the coupling \sqrt{R} , the fits prefer a somewhat larger value than the one used in ref.[21]. Next, we consider the scalar meson exchange. The pertinent parameters are $\bar{c}_{d,m}, M_S$ and g_S . For the constrained fits, we used $\bar{c}_m = \bar{c}_d = F_\pi/\sqrt{6} \pm 30\%$ and $M_S = 1200 \text{ MeV} \pm 30\%$, with the central values discussed above. Although these parameters are not very well constrained by the fits, we observe a few remarkable features. First, the scalar mass prefers to come out large, which essentially means that the scalar–isoscalar exchange can be very well represented by a contact term. Also, the product of the scalar couplings to the the nucleon and the pions in units of the scalar mass squared turns out to be essentially constant,

$$\frac{\bar{c}_m g_S}{M_S^2} \simeq (1.7 \dots 2.1) \cdot 10^{-3} \text{ MeV}^{-1} . \quad (5.4)$$

This number is about a factor of two larger than in ref.[11] pointing towards a larger LEC c_1 and consequently a larger pion–nucleon σ –term. However, it is known that there are sizeable fourth order corrections to the scalar sector of (HB)CHPT and we therefore do not want to dwell on this point any further. At first sight, these findings are in disagreement with meson–exchange models or K–matrix approaches which like to have a light scalar–isoscalar meson. Note, however, that due to our chirally symmetric construction, the $S\pi\pi$ coupling has a different momentum–dependence than what is usually assumed in these other approaches. To mimic this momentum–dependence, a light scalar is needed although the resulting fits are much worse in such case. For the ρ –meson, we have three parameters. The conventional ones are g_ρ and κ_ρ . From these, only κ_ρ is reasonably well determined, $\kappa_\rho = 6.1 \pm 0.4$ [36]. There is a larger spread in the values obtained for g_ρ either from the

width, the KFSR relation or fits to the nucleon electromagnetic form factors. To cope with this uncertainty and remembering again that we have no form factors at the vertices, in the constrained fits we limit g_ρ between 5 and 8. For example, the standard Höhler–Pietarinen analysis [37] gives $g_{\rho NN} = 5.7$. Note, however, that even in the fits without limits, g_ρ always stays in this range. On the contrary, the value of κ_ρ is not well determined by the unconstrained fits. The additional parameter T_+ is always negative and small. We introduce the dimensionless parameter $\tilde{T}_+ = (M^2 M_\rho^2)/(\sqrt{2} g_{\rho NN}) T_+$, and find $-0.3 \leq \tilde{T}_+ \leq -0.1$, i.e. the overall contribution of this additional term is small in most partial waves. In S_{11} and P_{13} , however, varying \tilde{T}_+ in the range mentioned leads to visible changes in the phase shifts, in particular above $W \simeq 1.2$ GeV. Therefore, it would be interesting to study the effect of this extra coupling in other approaches to πN scattering. The last parameter concerns the matching of the chiral amplitude to the unitarized amplitude at the subtraction point s_0 . Setting $\sqrt{s_0} = m + aM$, we always find that $a = 0.16$.

We now turn to the fits with $e_s = 0$. As already remarked, the Δ parameters are somewhat less well described, we get $g_{\pi\Delta N} = 2.25$, Z between -0.2 and -0.1 and $(m_\Delta, \Gamma_\Delta/2) = (1199, 58)$ MeV for the complex pole. On the contrary, the coupling \sqrt{R} of the Roper is consistent with the one given in ref. [21]. The results for the scalar and the ρ meson parameters are similar to the ones for $e_s = \sqrt{2}$, again we note that the combination of the scalar couplings lies in the narrow range of $(1.5 \dots 1.7) \cdot 10^{-3} \text{ MeV}^{-1}$. The matching of the chiral and unitarized amplitudes happens at larger values of $a \simeq 0.5$. This is, of course, expected and leads to an improved description of the S–wave scattering lengths as compared to the case of $e_s = \sqrt{2}$. In the following section, we will tabulate some of the numbers discussed here and also display some representative fits.

5.2 Representative fits

After having discussed the genuine results in the previous paragraph, we give in table 1 the values of the various fitted quantities for four representative fits with $e_s = \sqrt{2}$, based on the SM95 partial waves (using the KA84 analysis leads to very similar results). For all these fits, the χ^2/dof is very small. Although for the case of no limits on the parameters the χ^2/dof improves, these fits should only be considered illustrative since they lead to too large parameters in the scalar sector (we stress again that in such an approach as presented here one is only sensitive to products of couplings). The first fits are based on limiting the ranges allowed for the scalar couplings $\bar{c}_{d,m}$, the scalar mass and the ρ couplings. In fits 3,4 all these limits are lifted. Fits 2 and 4 differ from 1 and 3, respectively, in that the vector coupling G_V is reduced from 67 to 53 MeV (as explained before). The results are collected in table 1. The χ^2/dof is of similar quality in all these fits. Note the remarkable fact that in all the fits, also for the case of the second table, the a parameter is always less than 1, as required by our final definition of the $g(s)$ function, eq. (4.14). Note also that in the constrained fits, the product $\bar{c}_m \bar{c}_d$ comes out close to the large N_c result of $(38 \text{ MeV})^2$, cf. eq.(3.14), although individually \bar{c}_m (\bar{c}_d) prefers somewhat larger (lower) values than $F_\pi/\sqrt{6}$. The scalar mass always tends to the upper end of the given range. For these four fits, we find $\bar{c}_m g_S/M_S^2 = (2.1, 1.9, 1.7, 1.7) \cdot 10^{-3} \text{ MeV}^{-1}$, in order. If we, however, fix the scalar mass to 1200 MeV, \bar{c}_d comes out closer to the large N_c prediction and g_S is smaller, but again we find that the aforementioned product of scalar couplings is $1.7 \cdot 10^{-3} \text{ MeV}^{-1}$. As noted before, our fits are only sensitive to the products $G_V g_\rho$, $G_V \kappa_\rho$ and $G_V T_+$. This is reflected by the fact that for fits 3 and 4, we find the same value for $G_V g_\rho$ and almost the same for fits 1 and 2. The corresponding S– and P–wave phase shifts are shown in fig.9.

	Fit 1	Fit 2	Fit 3	Fit 4
$g_{\pi\Delta N}$	2.05	2.04	2.05	2.05
Z	-0.16	-0.08	-0.05	-0.05
\sqrt{R}	0.67	0.79	0.79	0.79
\tilde{T}_+	-0.15	-0.26	-0.09	-0.09
\bar{c}_d [MeV]	26.2 (25.,50.)	25.0 (25.,50.)	$5.9\cdot 10^5$	115.8
\bar{c}_m [MeV]	50.0 (25.,50.)	43.9 (25.,50.)	$1.0\cdot 10^6$	199.8
M_S [MeV]	1560 (840,1560)	1560 (840,1560)	$3.8\cdot 10^7$	63681.
g_S	100.2 [†]	104.3 [†]	$2.4\cdot 10^{6\dagger}$	35159. [†]
G_V [MeV]	67*	53*	67 *	53*
g_ρ	5.00 (5,8)	5.00 (5,8)	6.08	7.70
κ_ρ	5.70 (5.7,6.5)	5.70 (5.7,6.5)	3.53	3.53
a	0.16	0.16	0.16	0.16
χ^2/dof	21.5/355	15.6/355	12.9/355	12.0/355

Table 1: Representative fits with $e_s = \sqrt{2}$ as explained in the text. The * denotes a fixed quantity and the [†] indicates that g_S appears always multiplying $\bar{c}_{d,m}$. For fits 1,2, the ranges on the various parameters as explained in the text are given in the round brackets.

	Fit 1	Fit 2	Fit 3	Fit 4
$g_{\pi\Delta N}$	2.21	2.25	2.26	2.26
Z	-0.18	-0.12	-0.09	-0.09
\sqrt{R}	0.46	0.56	0.54	0.54
\tilde{T}_+	-0.19	-0.23	-0.08	-0.08
\bar{c}_d [MeV]	25. (25.,50.)	25.7 (25.,50.)	$5.7\cdot 10^5$	87847.
\bar{c}_m [MeV]	45.2 (25.,50.)	45.3 (25.,50.)	$1.0\cdot 10^6$	126.7
M_S [MeV]	1560 (840,1560)	1560 (840,1560)	$3.9\cdot 10^7$	222.5
g_S	92.6 [†]	87.9 [†]	$2.3\cdot 10^{6\dagger}$	53682. [†]
G_V [MeV]	67*	53*	67 *	53*
g_ρ	5.00 (5,8)	5.62 (5,8)	6.76	8.55
κ_ρ	5.7 (5.7,6.5)	5.7 (5.7,6.5)	3.64	3.64
a	0.65	0.41	0.51	0.51
χ^2/dof	1.15	1.00	0.78	0.78

Table 2: Representative fits with $e_s = 0$ as explained in the text. The * denotes a fixed quantity and the [†] indicates that g_S appears always multiplying $\bar{c}_{d,m}$. For fits 1,2, the ranges on the various parameters as explained in the text are given in the round brackets.

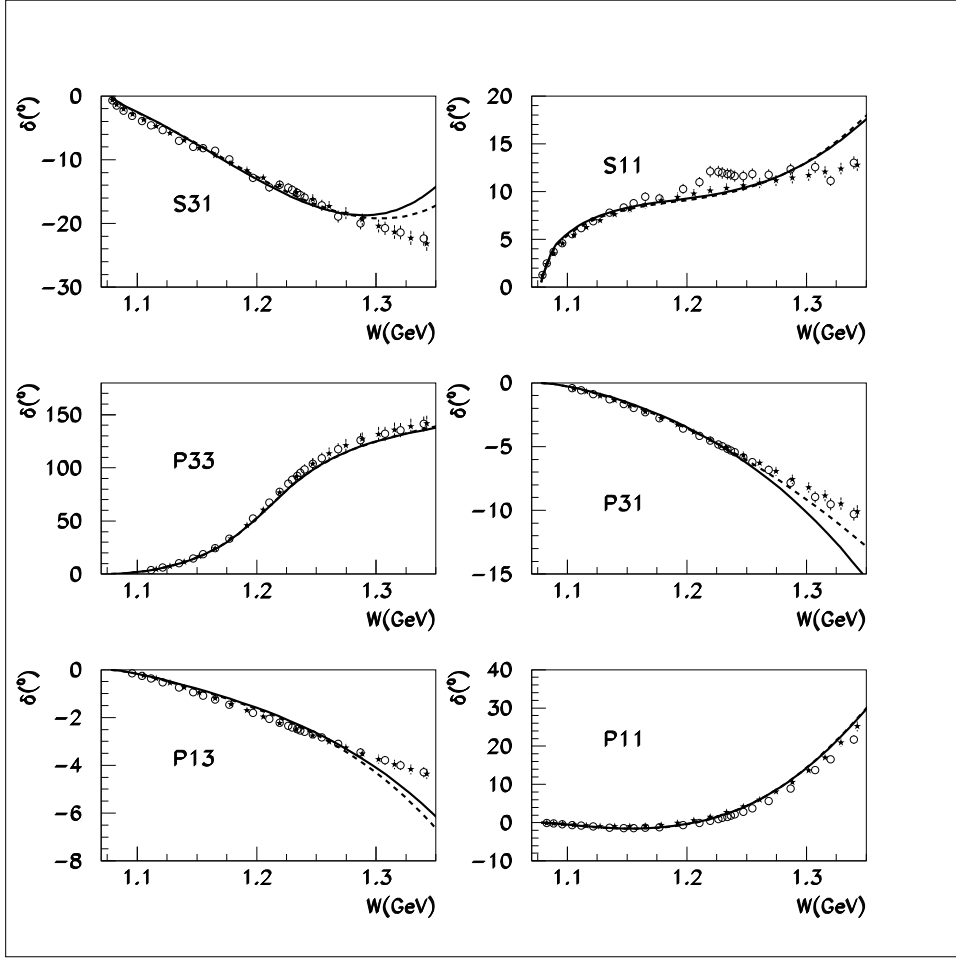


Figure 9: Fits to phase shifts as a function of the cm. energy W for $e_s = \sqrt{2}$ and $G_V = 53$ MeV. The solid (dashed) lines refer to the constrained (unconstrained) fits as described in the text.

We point out that in particular the P_{11} and the P_{33} partial waves are well described, and a good overall description of data up to $W = 1.3$ GeV is achieved. If one calculates the S-wave scattering lengths and the P-wave scattering volumes, these come out in reasonable agreement with the data.

We now turn to the fits with $e_s = 0$. We have performed the same four fits as described above. The resulting parameters are collected in table 2. These are similar to what was found before. The most striking differences are the Roper coupling, which comes out close to the value derived in ref.[20] and the larger value for the matching parameter a . Still, we find $a < 1$, as demanded by our definition of the matching function $g(s)$. The resulting χ^2/dof is around 1. Note that this number is only of limited meaning since it strongly depends on the choice of e_s , which now is 0 and for table 1 it was $\sqrt{2}$, and on the assumed statistical uncertainty. The resulting S- and P-wave scattering lengths (volumes) are collected in table 3. With the exception of a_{0+}^+ , they are in good agreement with the results based upon the Karlsruhe and VPI partial wave analysis. We stress that a_{0+}^+ is very sensitive to cancelations between contact term and loop contributions, which are individually much bigger than the total sum [41], and thus is only expected to be described precisely at fourth order. The resulting phase shifts for $W \leq 1.3$ GeV are shown in fig.10. They are slightly worse than the ones for the fits with $e_s = \sqrt{2}$. In particular, the P_{33} partial wave is not as precisely described as before, but still the complex pole is only slightly displaced as compared to the fits with $e_s = \sqrt{2}$.

Obs.	Fit 1	Fit 2	Fit 3	KA85	SP98
a_{0+}^+	1.59	1.13	0.87	-0.83	0.0 ± 0.1
a_{0+}^-	8.37	8.31	8.28	9.17	8.83 ± 0.07
a_{1-}^+	-4.92	-4.85	-5.03	-5.53	-5.33 ± 0.17
a_{1+}^+	13.71	13.87	13.73	13.27	13.6 ± 0.1
a_{1-}^-	-1.23	-1.27	-1.21	-1.13	-1.00 ± 0.10
a_{1+}^-	-8.08	-8.15	-8.10	-8.13	-7.47 ± 0.13

Table 3: Values of the S- and P-wave threshold parameters for the various fits as described in the text in comparison to the respective data (taken from ref.[1]). Fits 3 and 4 give identical results within the precision displayed. Units are appropriate inverse powers of the pion mass times 10^{-2} .

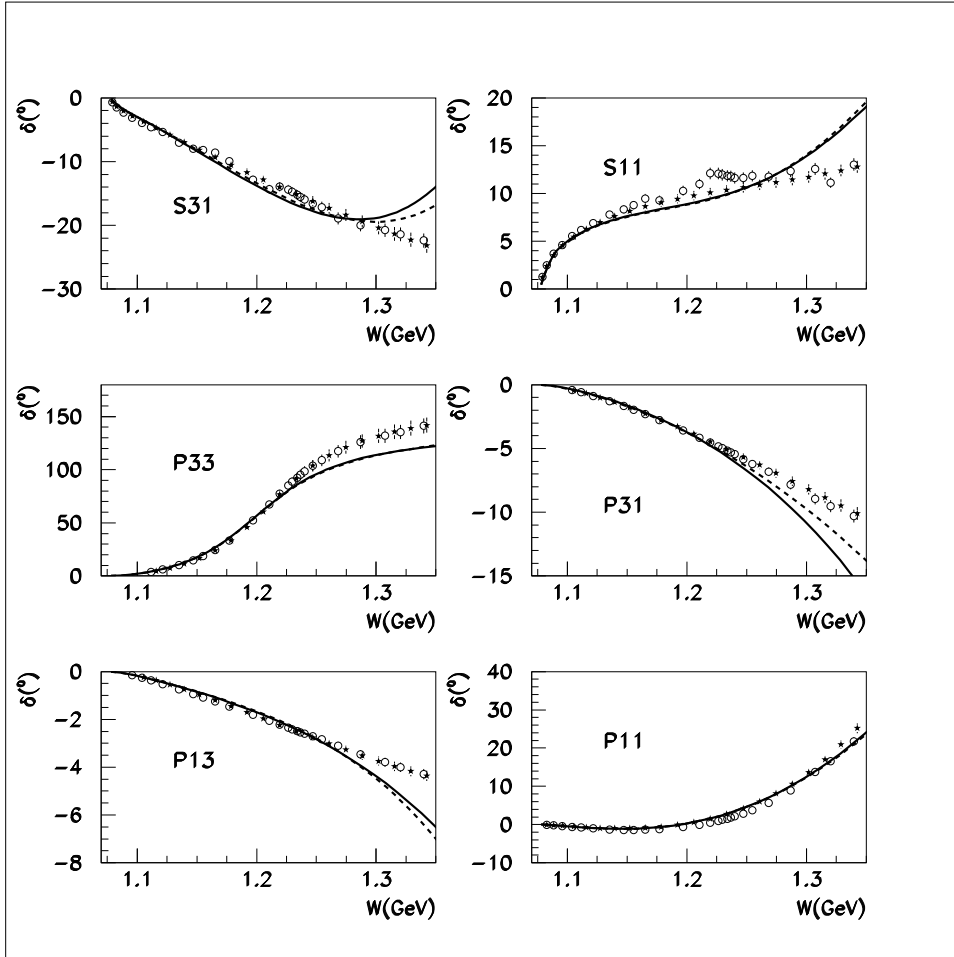


Figure 10: Fits to phase shifts as a function of the cm. energy W for $e_s = 0$ and $G_V = 53$ MeV. The solid (dashed) lines refer to the constrained (unconstrained) fits as described in the text.

6 Conclusions

In this paper, we have developed a novel chiral unitary approach for meson-baryon processes. As a first application, we have considered elastic pion–nucleon scattering from threshold up to the opening of the inelastic channels at $W \simeq 1.3$ GeV. Making use of the time-honored N/D method, we have derived the most general structure of any pion–nucleon partial wave amplitude neglecting unphysical cuts. The latter are then treated in a perturbative chiral loop expansion based on the power counting of heavy baryon chiral perturbation theory. The most important and novel features and results of this approach can be summarized as follows:

- i) The approach is based on subtracted dispersion relations and is by construction relativistic. No form factors, finite momentum cut-offs or regulator functions are needed to render the resummation finite. This is done by a subtraction of the dispersion relations below the physical threshold.
- ii) The amplitude is matched to the one of (heavy baryon) chiral perturbation theory at third order. This is done at an energy slightly below the physical threshold. In this region, the HBCHPT amplitude is expected to converge. It is straightforward to extend this matching to a fourth order and/or a relativistic CHPT amplitude.
- iii) The explicit resonance degrees of freedom contain free parameters (couplings and masses) which are determined from a best fit to the pion–nucleon partial waves. Some of these parameters, in particular the ones of the Δ , are very well determined. Couplings of the scalar and vector mesons can be pinned down less precisely. We have also pointed out a new coupling of the ρ not considered in conventional schemes. Our approach is consistent with the concept of resonance saturation of the low-energy constants.
- iv) The pion–nucleon phase shifts are well described below the onset of inelasticities. With the exception of the isoscalar S-wave scattering lengths, we also find a reasonable description of the πN threshold parameters. This can be improved by matching to a more precise (HB)CHPT amplitude.
- v) Our method is very general. It embodies (as a particular limiting case) the inverse amplitude method (IAM) [42] recently applied to the πN scattering in [43]. For a discussion about this point see refs. [10, 44]. The chiral unitary approach [7], based on the lowest order tree level meson–baryon interactions, appears also as a special case [44].
- vi) The extension of this approach to coupled channels (like $\pi N \rightarrow \eta N$) and to the three-flavor sector (with coupled channels) is in principle straightforward. For the kaon–nucleon system, the matching to the chiral perturbation theory amplitude is more tricky due to the appearance of subthreshold resonances. Work along these lines is in progress.

Acknowledgements

We are grateful to Nadia Fettes for some clarifying comments. This work was supported in part by the EEC-TMR program under contract no. ERBFMRX-CT98-0169.

References

- [1] N. Fettes, Ulf-G. Meißner and S. Steininger, Nucl. Phys. **A640** (1998) 199.
- [2] G. Höhler, in Landolt-Börnstein, Vol. 9b2, ed. H. Schopper (Springer, Berlin, 1983).
- [3] C. Schütz, J. Haidenbauer, J. W. Durso and J. Speth, Phys. Rev. **C57** (1998) 1464; O. Krehl, C. Hanhart, S. Krewald and J. Speth, 'What is the structure of the Roper resonance?', nucl-th/9911080.
- [4] P. F. A. Goudsmit, H. J. Leisi, E. Matsinos, B. L. Birbrair and A. B. Gridnev, Nucl. Phys. **A575** (1994) 673.
- [5] J. A. Oller and E. Oset, Phys. Rev. **D60** (1999) 074023.
- [6] N. Kaiser, P. B. Siegel and W. Weise, Nucl. Phys. **A594** (1995) 325.
- [7] E. Oset and A. Ramos, Nucl. Phys. **A635** (1998) 99.
- [8] T. R. Hemmert, B. R. Holstein and J. Kambor, J. Phys. **G24** (1998) 1831.
- [9] G. F. Chew and S. Mandelstam, Phys. Rev. **119** (1960) 467.
- [10] J. A. Oller, 'The Case of a WW Dynamical Scalar Resonance within a Chiral Effective Description of the Strongly Interacting Higgs Sector', to appear in Phys. Lett. **B**; hep-ph/9908493.
- [11] V. Bernard, N. Kaiser, Ulf-G. Meißner, Nucl. Phys. **A615** (1997) 483.
- [12] T. Becher and H. Leutwyler, Eur. Phys. J. **C9** (1999) 643.
- [13] V. Bernard, N. Kaiser and Ulf-G. Meißner, Int. J. Mod. Phys. **E4** (1995) 193.
- [14] Ulf-G. Meißner, Lectures given at 12th Annual HUGS at CEBAF, Newport News, VA, USA, 2-20 June, 1997; hep-ph/9711365.
- [15] P. Büttiker and Ulf-G. Meißner, 'Pion-nucleon scattering inside the Mandelstam triangle'; to appear in Nucl. Phys. **A**, hep-ph/9908247.
- [16] V. Bernard, N. Kaiser and Ulf-G. Meißner, Nucl. Phys. **B357** (1997) 129.
- [17] M. Mojzis, Eur. Phys. J. **C2** (1998) 181.
- [18] G. Ecker, J. Gasser, A. Pich and E. de Rafael, Nucl. Phys. **B321** (1989) 311.
- [19] B. Borasoy and Ulf-G. Meißner, Int. J. Mod. Phys. **A11** (1996) 5183.
- [20] B. Borasoy and Ulf-G. Meißner, Ann. Phys. NY **254** (1997) 192.
- [21] V. Bernard, N. Kaiser and Ulf-G. Meißner, Nucl. Phys. **B457** (1995) 147.
- [22] G. Höhler, πN Newsletter **9** (1993) 1.
- [23] G. Ecker, J. Gasser, H. Leutwyler, A. Pich and E. de Rafael, Phys. Lett. **B223** (1989) 425.
- [24] J. Gasser and H. Leutwyler, Nucl. Phys. **B250** (1985) 465, 517, 539.
- [25] M. Jamin, J. A. Oller and A. Pich, in progress.
- [26] J. A. Oller, E. Oset, Nucl. Phys. **A620** (1997) 438; (E) Nucl. Phys. **A652** (1999) 407.
- [27] G. Janssen, B. C. Pearce, K. Holinde and J. Speth, Phys. Rev. **D52** (1995) 2690.
- [28] Ulf-G. Meißner, Comm. Nucl. Part. Phys. **20** (1991) 119.
- [29] S. Peris, M. Perrottet and E. de Rafael, JHEP **9805** (1998) 011; A. A. Andrianov, D. Espriu and R. Tarrach, Nucl. Phys. **B533** (1998) 429.
- [30] Frang Shi, T. G. Steele, V. Elias, K. B. Sprague, Ying Xue, A. H. Fariborz, 'Hoelder Inequalities and Isospin Splitting of the Quark Scalar Mesons'; hep-ph/9909475.
- [31] L. Castillejo, R. H. Dalitz and F. J. Dyson, Phys. Rev. **101** (1956) 453.

- [32] G. t'Hooft, Nucl. Phys. **B72** (1974) 461; Nucl. Phys. **B75** (1974) 461; E. Witten, Nucl. Phys. **B160** (1979) 57.
- [33] N. Fettes, Ulf-G. Meißner and S. Steininger, JHEP **9809** (1998) 008.
- [34] M. Benmerrouche, R. M. Davidson and N. C. Mukhopadhyay, Phys. Rev. **C39** (1989) 2339.
- [35] V. Bernard, N. Kaiser and Ulf-G. Meißner, Z. Phys. **C70** (1996) 483.
- [36] P. Mergell, Ulf-G. Meißner and D. Drechsel, Nucl. Phys. **A596** (1996) 367.
- [37] G. Höhler and E. Pietarinen, Nucl. Phys. **B95** (1975) 210.
- [38] R. Koch, Z. Phys. **C29** (1985) 597.
- [39] R. A. Arndt, I. I. Strakovsky, R. L. Workman and M. M. Pavan, Phys. Rev. **C52** (1995) 2120.
- [40] O. Hanstein, D. Drechsel and L. Tiator, Phys. Lett. **B385** (1996) 45.
- [41] V. Bernard, N. Kaiser and Ulf-G. Meißner, Phys. Lett. **B309** (1993) 421.
- [42] T. N. Truong, Phys. Rev. Lett. **61** (1998) 2526; Phys. Rev. Lett. **67** (1991) 2260; A. Dobado, M. J. Herrero and T. N. Truong, Phys. Lett. **B235** (1990) 134; A. Dobado and J. R. Peláez, Phys. Rev. **D47** (1993) 4883; Phys. Rev. **D56** (1997) 3057; J. A. Oller, E. Oset and J. R. Peláez, Phys. Rev. Lett. **80** (1998) 3452; J. A. Oller, E. Oset and J. R. Peláez, Phys. Rev. **D59** (1999) 74001; (E) Phys. Rev. **D60** (1999) 099906.
- [43] J. R. Peláez and A. Gómez Nicola, 'The Inverse Amplitude Method and Heavy Baryon Chiral Perturbation Theory applied to pion-nucleon scattering'; hep-ph/9909568.
- [44] J. A. Oller, E. Oset and A. Ramos, 'Chiral Unitary approach to meson-meson and meson-baryon interactions and nuclear applications', forthcoming.